JOURNAL OF APPLIED ELECTROCHEMISTRY 24 (1994) 685–693

Electrochemical study of mass transfer in decaying annular swirl flow
Part 1: Axial distribution of local mass transfer coefficients

S. YAPICI*, M. A. PATRICK, A. A. WRAGG

School of Engineering, Exeter University, North Park Rd., Exeter, EX4 4QF, Great Britain

Received 11 October 1993; revised 26 January 1994

This paper describes an investigation of local mass transfer behaviour at the inner rod and outer pipe wall of an annular test section in decaying annular swirl flow generated by axial vane-type swirl generators. Four swirl generators with vane angles of between 15–60° to the axis of the duct were used. The experiments were carried out in the Reynolds number range 3300–50 000 and at a Schmidt number of 1650. The axial distribution of the local mass transfer coefficients at both the inner rod and the outer wall were measured using an electrochemical technique. Current fluctuations were also recorded to gain information on the turbulence characteristics in the vicinity of the local electrodes.

Nomenclature

D	diffusion coefficient ($m^2\ s^{-1}$)
d	duct diameter (m)
k	mass transfer coefficient ($m\ s^{-1}$)
L	axial length (m)
x	axial distance (m)
$(\overline{vw})_w$	tangential stress coefficient [25]
$(\overline{uv})_w$	axial stress coefficient [25]

Dimensionless groups

Re	Reynolds number $(Ud/\nu), (Ux/\nu)$
Sc	Schmidt number (ν/D_{AB})

Greek symbols

α	annulus ratio
θ	vane angle (degree)
ν	kinematic viscosity ($m^2\ s^{-1}$)
ρ	density ($kg\ m^{-3}$)

Subscripts and superscripts

a	fully developed axial value
e	equivalent
i	inner rod
o	outer wall
s	swirl flow
w	wall

1. Introduction

Enhancement of convective heat and mass transfer in process equipment is sought because of the necessity for energy and material savings. Many techniques are known to be effective in enhancing convective transfer rates. These can be divided into two main groups: passive techniques and active techniques. Passive techniques include the use of treated surfaces, rough surfaces, extended surfaces, swirl flow devices and coiled tubes. Active techniques, which require an extra external power source, include surface vibration, fluid vibration, electrostatic fields, injection or suction of fluid and jet impingement (Bergles and Webb [1], Reay [2]). Enhancement in the convective processes is obtained at the expense of energy dissipated by further friction, caused by non-smooth surfaces and insertions, or by the necessary external power. Decaying swirl flow is likely to be a promising means for enhancing convective heat and mass transfer, in terms of energy cost.

In swirl flow, the tangential velocity component, due to imposed concentric circular motion about the duct axis is of comparable magnitude to the mean axial flow velocity. Swirl flow in pipes may be usefully classified into two types: (i) continuous swirl flow and (ii) decaying swirl flow. In continuous swirl flow, the swirling motion is maintained over the whole length of the duct, while in decaying swirl flow, the swirl is generated at the entry section of the duct and decays along the flow path. King *et al.* [3] classified decaying swirl flows into three groups according to their surrounding boundaries:

(a) unconfined swirling flows, such as rotary gas burners, swirling free jets, and swirling compressible flows, for which the boundary layer effects are negligible;
(b) swirling flow in short, large diameter chambers

This paper was presented at the International Workshop on Electrodiffusion Diagnostics of Flows held in Dourdan, France, May 1993.

* Present address: Atatürk Üniversitesi, Mühendislik Fakültesi, Kimya Müh. Böl., 25240 Erzurum, Türkiye/Turkey.

0021-891X

where end-wall effects interact with the swirling motion to produce strong secondary flow effects, such as core-flow containment in gaseous nuclear rockets; (c) swirling flows in long, small diameter tubes where circumferential wall effects interact strongly with the swirling flow.

The present research is concerned with the distribution of local mass transfer in decaying swirl flow in a long, small diameter annular system.

The enhancement of heat transfer in decaying swirl flow has received considerable attention while very little is known about mass transfer in this type of flow. Pipe-flow heat transfer in decaying swirl flow has been investigated by Ivanova [4], using rotating axial vanes to generate swirl, Blackwelder and Kreith [5], and Klepper [6], who employed twisted tapes to obtain decaying swirl flow. Blum and Oliver [7], Hay and West [8], Sparrow and Chaboki [9], Lin *et al.* [10], investigated heat transfer in decaying swirl flow generated by tangential inlets. Koval'nogov and Shchukin [11], Narazhnyy and Sudarev [12], and Sudarev [13] investigated heat transfer in decaying swirl flow using axial-guide vane type swirlers. Most of the above workers employed smooth circular pipes as the test section; only Sudarev [13] used an annular geometry. The results of Ivanova [4] differ from other local swirl flow heat transfer results, which commonly have a decaying axial distribution, by displaying a peak in the entrance region. Dellenback *et al.* [14] studied local heat transfer in decaying swirl flow through an abrupt expansion and found that increasing swirl intensity increased the maximum peak heat transfer sharply and that the enhancement in the peak values increased with decreasing Reynolds number, in the Reynolds number range 30 000–100 000.

Only a few studies have been reported in the literature on mass transfer in decaying swirl flow. Shoukry and Shemilt [15] investigated mass transfer enhancement in decaying swirl flow in an annular pipe generated by a single tangential inlet, using the electrochemical limiting diffusion current technique to measure average mass transfer coefficients. Nickel cathode rods at three different axial locations were employed. These workers found that a smaller tangential inlet diameter gave higher enhancement in mass transfer due to the larger tangential velocities. The mass transfer enhancement decreased with axial distance. De Sa *et al.* [16] extended the above study to the investigation of mass transfer in the entrance region of decaying annular swirl flow using rod cathodes of different lengths. They found that the mass transfer was higher than that in axial flow, for $Re > 6000$, and smaller for $Re < 6000$. Legentilhomme and Legrand [17, 18], carried out a very similar study to the above, including the effect of varying annulus ratio. It was found that the effect of initial swirl intensity, which was defined as the ratio of the fluid velocity in the tangential inlet duct to that in the annular gap, is negligible, and varying annulus ratio has little effect on the mass transfer process in decaying annular swirl flow. These workers also found that, with tangential inlet diameters smaller than or equal to the annular gap, mass transfer was higher than for tangential inlet diameters larger than the annular gap.

Table 1. Electrolyte physical properties at 20° C

ρ/kg m^{-3}	1020
μ/kg m^{-1} s^{-1}	1.11×10^{-3}
D_{ferri}/m^2 s^{-1}	6.601×10^{-10}
D_{ferro}/m^2 s^{-1}	5.02×10^{-10}
Sc	1650

Table 2. Swirler geometries

Designed angle/degree	*Actual angle/degree*		*Total axial length of swirler/mm*
	θ_i	θ_o	
15	15	16	32
30	31	34	28
35	35.5	39	26
45	45.3	50	21
60	61.5	67	13

The mass transfer studies described above do not provide information on truly local mass transfer behaviour. The present study was prompted by the need for further work on mass transfer in decaying swirl flow with emphasis on fuller understanding of local characteristics. A preliminary account showing visualisation of swirl flow patterns using a dye-trace technique and presenting pressure drop data across the swirl generators used in the present work, together with some limited mass transfer data, has already been presented [23].

2. Experimental techniques

Full details of the experimental technique and test section construction can be found in [19]. For the mass transfer measurements the electrochemical limiting diffusion current technique was employed. The electrode/electrolyte system used was the potassium ferri-ferrocyanide couple supported with sodium hydroxide and a nickel anode and cathode. The test fluid temperature was maintained constant at 20° C within ∓ 0.5° C, using a coated coil immersed in the electrolyte reservoir. The physical properties of the electrolyte solution at 20° C are given in Table 1. All piping sections were made of PVC to ensure chemical inertness to the test electrolyte, and to avoid the adverse effects of light.

Four short annular axial-vane swirl generators were manufactured from PVC rod of 12 mm diameter and PVC sheet of 1 mm thickness with nominal blade angles of 15, 30, 45 and 60° to the pipe axis.* The geometric characteristics of the swirl

* Due to imperfections in manufacture the actual resultant inner and outer angles of the blades differed from the nominal. The actual values of θ_i and θ_o are given in Table 2 and these actual values are also in the legends to Figs 5–8.

generators are given in Table 2. The whole length of experimental section was approximately 100 equivalent diameters; 50 equivalent diameters of this was entry section, which was made of 12 mm PVC rod and 26.6 mm ID perspex pipe, with the remaining part as the test section. In the case of axial annular flow with no swirl, a length of about 35 equivalent diameters is necessary to obtain fully developed flow (Brighton and Jones [20]). Thus, a fully developed annular flow was obtained before the test section for all experiments. The inner rod electrode was made of 12 mm diameter 99.99% pure nickel rod of 765 mm length having 32 nickel local electrodes of 1 mm diameter at 23 mm intervals, giving about 50 equivalent diameters length. A nickel outer pipe of 26.6 mm ID and of the same length as the inner rod was used as the counter electrode. For the mass transfer measurements at the outer wall, a nickel pipe of 26.6 mm ID and 500 mm length having 32 local electrodes of 1 mm diameter, at 14 mm intervals, giving approximately 32 equivalent diameters length, was constructed as the cathode system.

Current fluctuations were recorded from selected local electrodes in order to observe the turbulence characteristics of the local mass transfer rate. The fluctuations recorded in this way represent fluctuations in the rate of mass transfer to a finite area, not to a true point [21].

For the mass transfer measurements, the necessary preparatory steps to ensure the most accurate possible measurements, as reviewed by Berger and Ziai [22], were applied.

3. Results and discussions

3.1. *Local mass transfer measurements*

The axial distributions of the local mass transfer coefficients for the 15 and 60° swirl generators are given in Figs 1 and 2 for the inner rod, and in Figs 3 and 4 for the outer wall, respectively. The axial distribution of the local mass transfer enhancement in terms of the ratio of the Sherwood numbers for swirl flow to the Sherwood number for fully developed annular flow with no swirl downstream

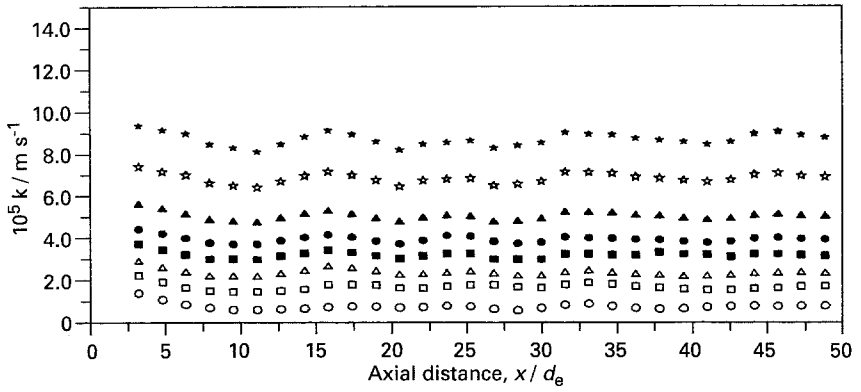

Fig. 1. Axial distribution of the local mass transfer coefficients downstream of the 15° swirler for the inner rod at different Reynolds numbers: (○) 3350, (□) 7420, (■) 10 260, (●) 18 520, (▲) 25 370, (☆) 37 140, (★) 50 600.

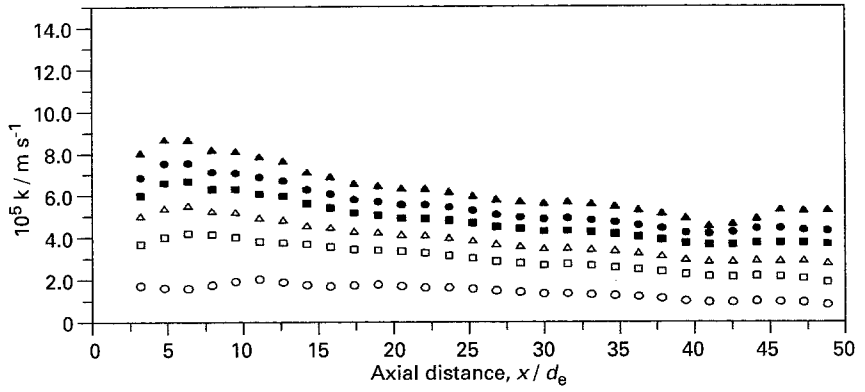

Fig. 2. Axial distribution of the local mass transfer coefficients downstream of the 60° swirler for the inner rod at different Reynolds numbers: (○) 3350, (□) 7420, (△) 10 260, (■) 14 410, (●) 18 520, (▲) 25 370.

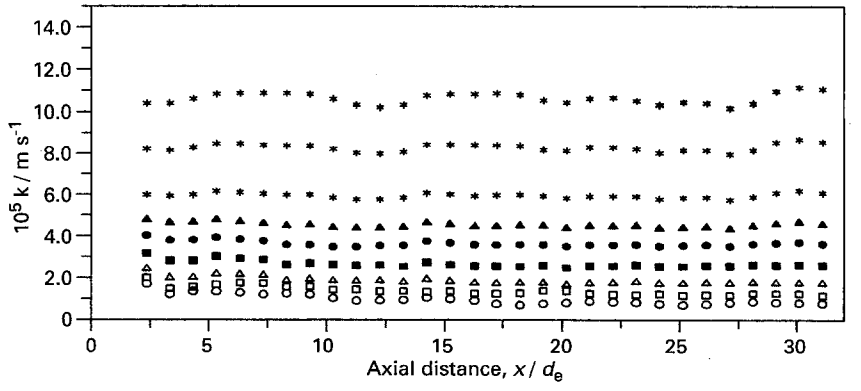

Fig. 3. Axial distribution of the local mass transfer coefficients downstream of the 15° swirler for the outer pipe at different Reynolds numbers: (○) 3350, (□) 5120, (△) 7420, (■) 10 260, (●) 14 410, (▲) 18 520, (*) 25 370, 37 140 and 50 630.

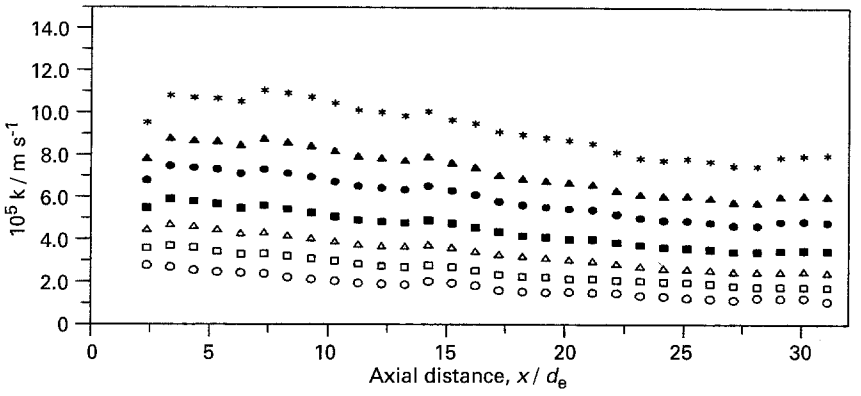

Fig. 4. Axial distribution of the local mass transfer coefficients downstream of the 60° swirler for the outer pipe at different Reynolds numbers: (○) 3350, (□) 5120, (△) 7420, (■) 10260, (●) 14410, (▲) 18520, (*) 25370.

of the four swirl generators, at Reynolds numbers of 3350 and 25370, are given in Figs 5 and 6 for the inner rod and in Figs 7 and 8 for the outer wall, respectively. The graphs of the axial distribution of local mass transfer coefficient in general show a decay in the axial direction which becomes more pronounced as the swirler angle increases. For low swirler angles the axial distributions show a periodic behaviour. This is especially pronounced at higher Reynolds numbers. The enhancement in the local mass transfer coefficients, compared to values in fully developed annular flow, is higher at higher swirler angles and lower Reynolds numbers. For the 60° swirler, at a Reynolds number of about 3300, the

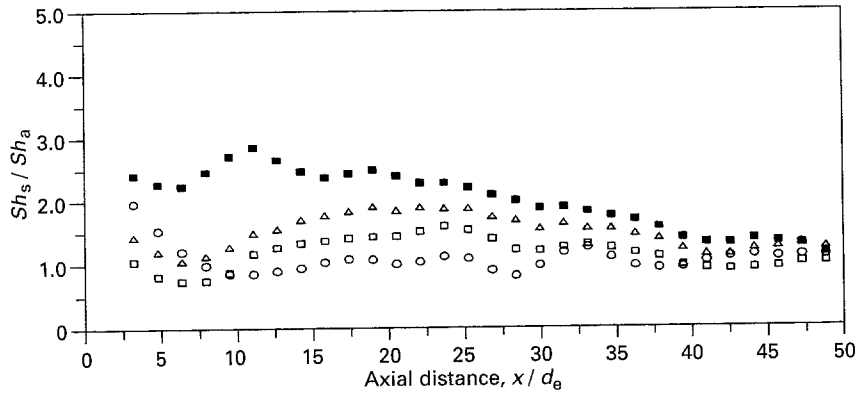

Fig. 5. Axial distribution of the relative local mass transfer enhancement for four swirlers for the inner rod at $Re = 3350$. Swirl angle: (○) 15°, (□) 31°, (△) 45.3°, (■) 61.5°.

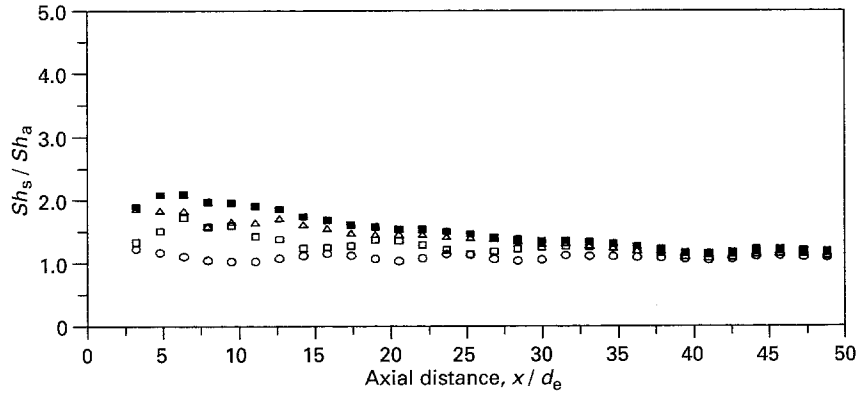

Fig. 6. Axial distribution of the relative local mass transfer enhancement for four swirlers for the inner rod at $Re = 25370$. Swirl angle: (○) 15°, (□) 31°, (△) 45.3°, (■) 61.5°.

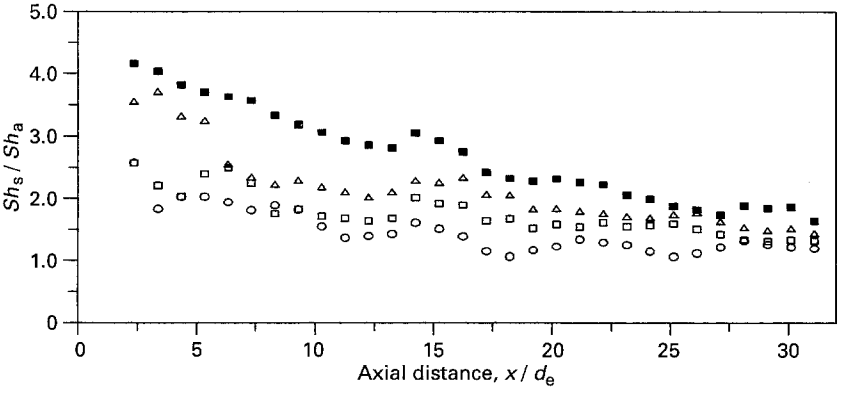

Fig. 7. Axial distribution of the relative local mass transfer enhancement for four swirlers for the outer pipe at $Re = 3350$. Swirl angle: (○) 16°, (□) 34°, (△) 50°, (■) 67°.

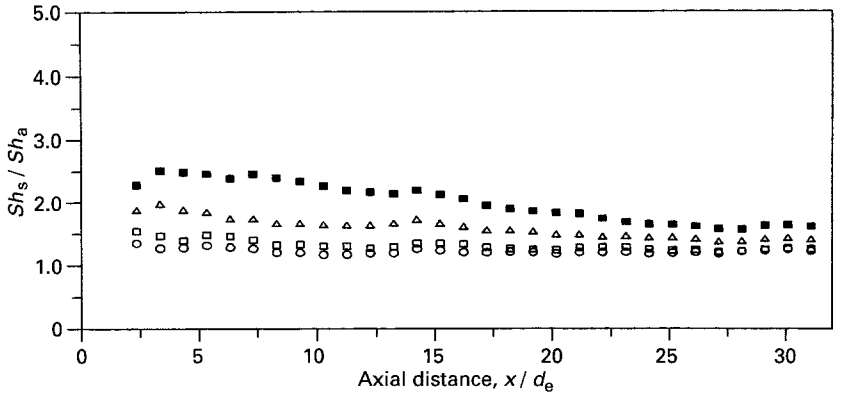

Fig. 8. Axial distribution of the relative local mass transfer enhancement for four swirlers for the outer pipe at $Re = 25\,370$. Swirl angle: (○) 16°, (□) 34°, (△) 50°, (■) 67°.

mass transfer coefficients reach values of approximately 2.8 times and 4.1 times those of fully developed annular flow, at the inner rod and the outer wall, respectively. The mass transfer coefficients decay towards the value for fully developed flow as the axial distance increases, but, even at 50 equivalent diameters downstream, the effect of swirl is still evident. The enhancement level in the mass transfer coefficient for the outer wall is higher than that for the inner rod, even allowing for the difference in the angles, given in Table 2, at the inner and outer edges of the vanes. Flow studies from the literature, Scott and Rask [24], Clayton and Morsi [25], and Yowakim and Kind [26], indicate that maximum axial velocities generally occur closer to the inner wall of the annulus and maximum tangential velocities always occur closer to the inner walls. Correspondingly, the positions of zero axial and tangential shear stress are generally located closer to the inner wall. However, Fig. 9 confirms that the values of the local mass transfer coefficient at the outer wall are higher than those at the inner wall, for the 30° generator and at a Reynolds number of 37 140.

Storck and Coeuret [27], in their study on mass and momentum transfer at a wall with turbulence promoters, found that mass transfer coefficients and shear stresses at the wall show parallel behaviour. Figure 10 shows the comparison between the behaviour of the axial distribution of the mass transfer coefficients at the inner wall and the outer wall of this study and the axial distribution of wall shear stresses for annular swirling flows from Scott and Rask [24] and from Clayton and Morsi [25]. The differences in the axial distributions of the measured quantities, shown in Fig. 10, reflect the geometry of the swirl generators which have a determinant effect on the flow behaviour, especially immediately downstream (Chigier and Beer [28], Bradshaw [29]). Scott and Rask [24] used radial inlet guide-vanes without any settling section before the test section. The fluid introduced directly into

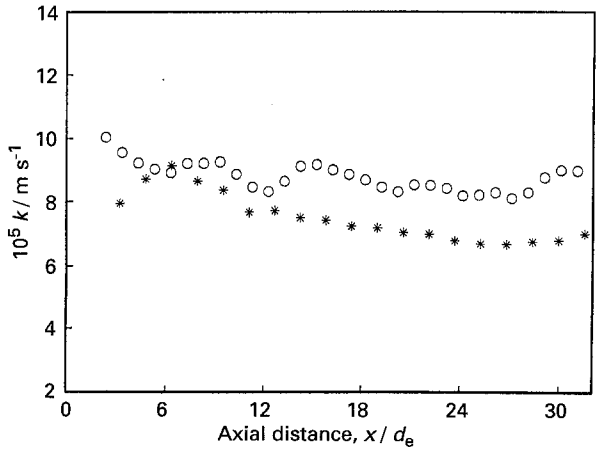

Fig. 9. Axial distributions of mass transfer coefficients at the inner rod (*) and the outer wall (○) for the 30° swirler at $Re = 37\,140$.

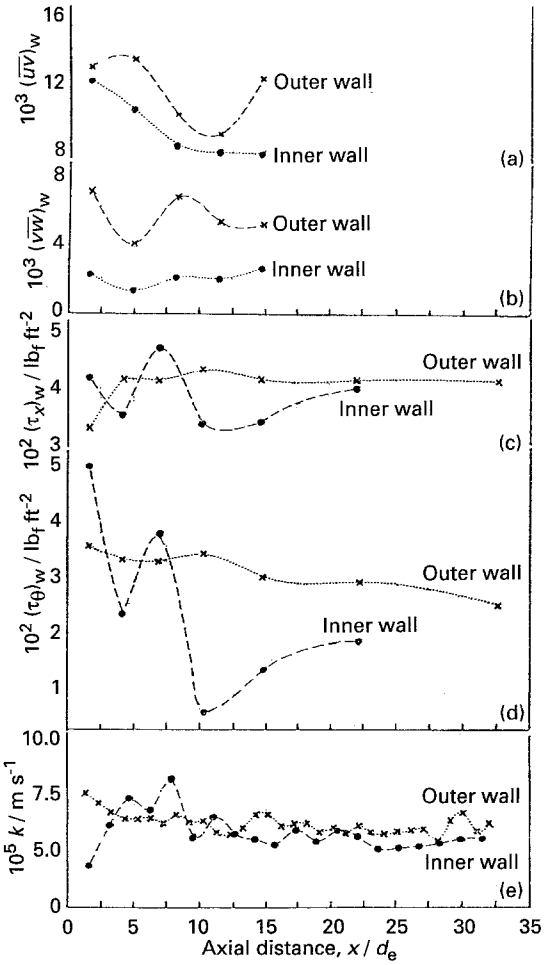

Fig. 10. Comparison of axial distribution of wall shear stresses from Clayton and Morsi [25]: (a) axial, (b) tangential wall shear stress, and from Scott and Rask [24]: (c) axial, (d) tangential wall shear stress, with (e) axial mass transfer distribution of the present study. (a) and (b): $\theta = 30°$, $\alpha = 0.51$, $Re = 28\,700$ with radial guide vanes. (c) and (d): $\theta = 45°$, $\alpha = 0.4$, $Re = 130\,000$ with radial guide vanes. (e): $\theta_i = 31°$, $\theta_o = 34°$, $\alpha = 0.45$, $Re = 25\,368$.

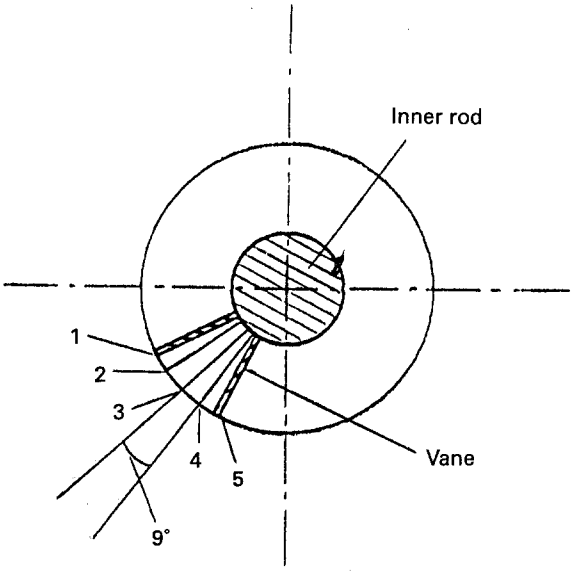

Fig. 11. Circumferential positions of local electrodes between adjacent swirler vanes.

the test section, radially through the vanes, hit the inner wall causing complex flow patterns and giving periodic behaviour in the axial distribution of the wall shear stress along the inner wall. Clayton and Morsi [25] used a bellmouth to introduce the swirl flow into a settling section, with as little disturbance as possible, and orifices at the end of the settling section to remove the wall layers built up at the bellmouth and the walls of the settling section. As seen from the figure these precautions avoided disturbances at the inner wall but could not avoid the generation of some disturbances at the outer wall, in contrast to the results of Scott and Rask. Aouabed *et al.* [30] observed similar periodic behaviour for the wall velocity gradient, especially on the inner wall, in decaying annular swirl flow generated by a single tangential inlet.

For the higher swirl angles, the axial distributions of the local mass transfer coefficients indicate a peak downstream of the swirl generator. In the literature, only Ivanova [4] has recorded similar behaviour for the axial distribution of heat transfer in decaying swirl flow. A peak in the local mass transfer rate is a characteristic feature observed downstream of an abrupt expansion (e.g. Choukhi *et al.* [31]). Dellenback *et al.* [14] also showed that swirl has a substantial effect in increasing the peak transfer rate downstream of such an expansion. The occurrence of a peak and the complex behaviour of the axial distribution of the mass transfer, especially at the inner rod, in the swirl flow of this study can be attributed to the occurrence of reverse flow due to high swirl, the eddies behind the vanes and the expansion of the flow cross section downstream of the obstruction due to the vanes of the swirl generator. This behaviour appears for swirl generators with higher angles, more obviously at the inner rod, since the possibility of internal reverse flow occurring due to higher swirl intensity and the effective expansion in cross section downstream of the obstruction due to the vanes of the swirler increases as the swirler angle increases. Legentilhomme and Legrand [18] also recorded similar behaviour in their study of mass transfer in annular decaying swirl flow with a single tangential inlet when they used tangential inlets having diameters smaller than the size of the annular gap.

3.2. *Circumferential mass transfer measurements*

To test for the influence of the relative position of the micro-electrodes to the individual vanes of a swirl generator, a further series of experiments was carried out. The local mass transfer coefficients were recorded at five different circumferential positions, as shown in Fig. 11.† The circumferential variation in the mass transfer measurements between two adjacent vanes is shown in Figs 12 and 14 for the 15° swirler and in Figs 13 and 15 for the 60° swirler, at a Reynolds number of 25 370, for the inner rod and the outer wall, respectively. Downstream of the swirl generator (up to approximately 10 equivalent diameters length) the behaviour of local mass transfer coefficients has a complex character for vane angles of 30° and over (as typified by Figs 13 and 15), especially at the inner rod. Thus, the effect of the position of the vanes relative to the point electrodes is more pronounced at the inner rod at high θ. However, for the 15° swirler the relative position of the vanes hardly affects the measurement of the axial mass transfer distribution at the inner wall.

3.3. *Current fluctuations*

Current fluctuations at the inner rod from selected point electrodes are shown in Fig. 16 for the 45° swirl generator at a Reynolds number of 25 370.

† In the results shown earlier (Figs 1–4) the circumferential position of the line of microelectrodes was not controlled.

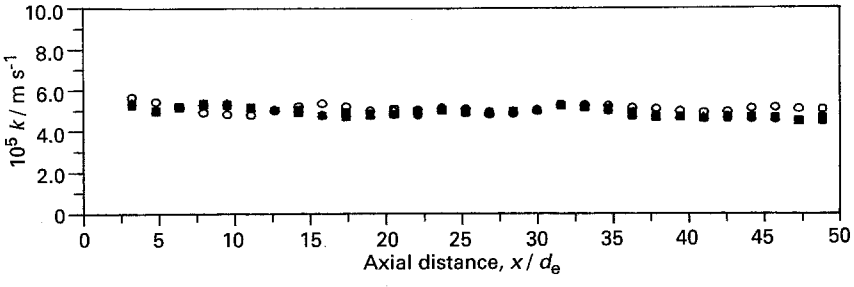

Fig. 12. Axial distribution of local mass transfer coefficients at five different circumferential locations between adjacent vanes for the 15° swirler for the inner rod at $Re = 25\,370$. Circumferential position: (○) Data from Fig. 1, (□) 1, (△) 2, (■) 3, (●) 4, (▲) 5.

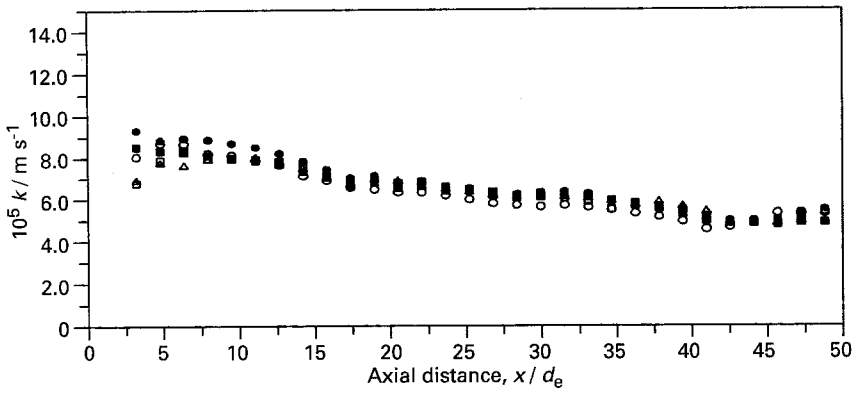

Fig. 13. Axial distribution of local mass transfer coefficients at five different circumferential locations between adjacent vanes for the 60° swirler for the inner rod at $Re = 25\,370$. Circumferential position: (○) Data from Fig. 2, (□) 1, (△) 2, (■) 3, (●) 4, (▲) 5.

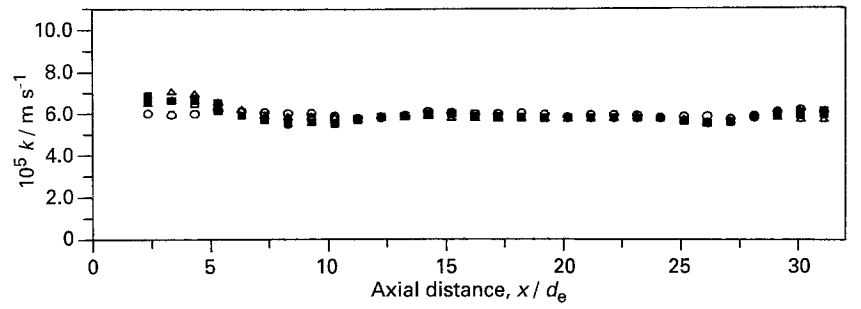

Fig. 14. Axial distribution of local mass transfer coefficients at five different circumferential locations between adjacent vanes for the 15° swirler for the outer wall at $Re = 25\,370$. Circumferential position: (○) Data from Fig. 3, (□) 1, (△) 2, (■) 3, (●) 4, (▲) 5.

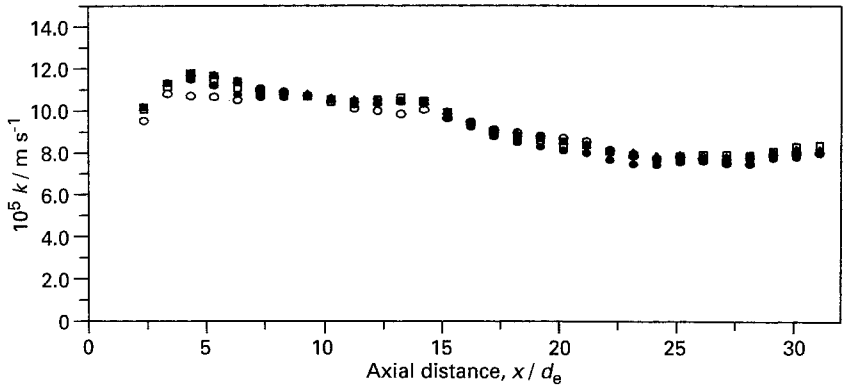

Fig. 15. Axial distribution of local mass transfer coefficients at five different circumferential locations between adjacent vanes for the 60° swirler for the outer wall at $Re = 25\,370$. Circumferential position: (○) Data from Fig. 4, (□) 1, (△) 2, (■) 3, (●) 4, (▲) 5.

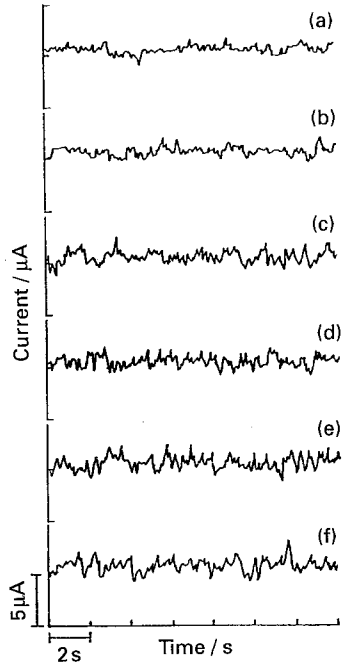

Fig. 16. Current fluctuations at different axial distances (x/d_e) downstream of the 45° swirler for the inner rod at $Re = 25\,370$. x/d_e: (a) 1.64, (b) 3.21, (c) 7.93, (d) 15.80, (e) 31.53 and (f) 47.26.

For the outer wall the current fluctuations for all swirl generators and for flow without swirl are given in Fig. 17, and more detail for the 60° swirler is given in Fig. 18. It is necessary to use a micro electrode having a diameter smaller than the smallest turbulent scales to provide good frequency response and to avoid averaging over the electrode surface, Mao and Hanratty [32]. Therefore, the recorded fluctuations here give a reasonable idea of turbulent behaviour. As can be seen from Fig. 17 there is suppression in the fluctuations in the entrance region as the swirler angle increases; the fluctuations revert to normal behaviour corresponding to the fully developed axial annular flow further downstream. The fluctuations at the inner rod generally show similar features but with rather less turbulence suppression in the entry region. However, the inner rod behaviour is distinctly more complex than that of the outer [19].

4. Conclusions

For the experimental conditions of the present study the following conclusions are made.

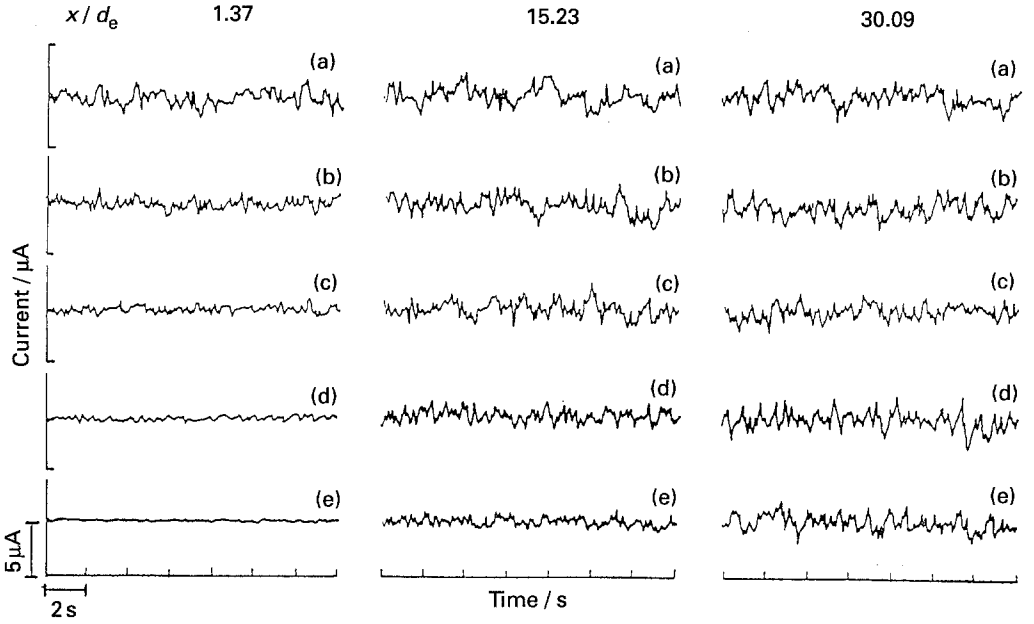

Fig. 17. Current fluctuations for the four swirlers at three downstream distances for the outer wall at $Re = 25\,370$. Swirler angles: (a) 0°, (b) 16°, (c) 34°, (d) 50° and (e) 67°.

(i) The decay rate of local mass transfer coefficients in the axial direction in an annular duct is higher at high swirler angles.
(ii) Relative mass transfer enhancement is greater at high swirler angles and low Reynolds numbers.
(iii) In the region immediately downstream of the swirl generator, the distribution of local mass transfer coefficients has a complex structure, especially for the inner rod. With small swirler angles, the axial distribution of the local mass transfer coefficient displays periodic behaviour.
(iv) For high swirler angles the axial distribution of local mass transfer coefficient tends to give a local peak.
(v) Current fluctuations are suppressed at high Reynolds numbers and high swirler angles at both walls, but more obviously so at the outer wall.

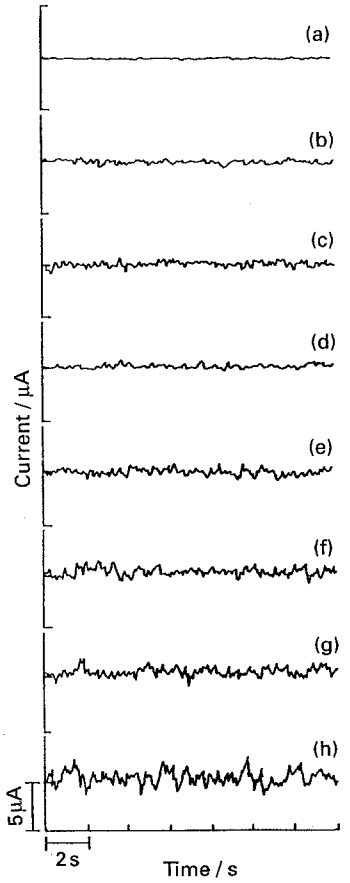

Fig. 18. Current fluctuations at different axial distances downstream of the 60° swirler for the outer wall at $Re = 25\,370$. x/d_e: (a) 1.37, (b) 2.36, (c) 4.34, (d) 5.33, (e) 7.31, (f) 10.28, (g) 15.23 and (h) 30.09.

References

[1] A. E. Bergles and R. L. Webb, *Adv. in Enhanced Heat Trans.*, HTD **43** (1985) 81.
[2] D. A. Reay, *Heat Recovery Sys. CHP* **11** (1991) 1.
[3] M. K. King, R. R. Rothfus and R. I. Kermode, *AIChE J.* **15** (1969) 837.
[4] A. Ivanova, Proceedings of the second all-Soviet Union conference on *Heat and Mass Transfer*, Minsk, **1** (1964) p. 243.
[5] R. Blackwelder and F. Kreith, 'Augmentation of Convective Heat and Mass Transfer', (edited by A. B. Bergles and R. L. Webb), American Society of Mechanical Engineers (1970).
[6] O. H. Klepper, *Heat Transfer, AIChE Symp. Ser.* **69** (1973) 87.
[7] F. A. Blum and L. R. Oliver, ASME Paper No. 66-WA/HT-62 (1975).
[8] H. Hay and P. D. West, *J. Heat Transfer, Trans. ASME* **97** (1975) 411.
[9] E. M. Sparrow and A. Chaboki, *ibid.* **106** (1984) 766.
[10] S. Lin, J. Chen and G. H. Vatistas, *Canadian J. Chem. Engng.* **8** (1990) 944.
[11] A. F. Koval'nogov and K. Shchukin, *J. Eng. Phys.* **14** (1968) 239.
[12] E. G. Narazhnyy and A. Sudarev, *Heat Transf.—Sov. Res.* **3** (1971) 62.
[13] A. Sudarev, *J. Eng. Phy.* **15** (1972) 1049.
[14] P. A. Dellenback D. E. Metzger and G. P. Neitzel, *J. Heat Transfer, Trans. ASME* **109** (1978) 613.
[15] E. Shoukry and L. W. Shemilt, *Ind. Eng. Chem. Process Des. Dev.* **24** (1985) 53.
[16] M. S. de Sa, E. Shoukry and I. V. Sogiarto, *Canadian J. Chem. Eng.* **69** (1991) 294.

[17] P. Legentilhomme and J. Legrand, *J. Appl. Electrochem.* **20** (1990) 216.
[18] *Idem, Int. J. Heat and Mass Transf.* **35** (1991) 12–81.
[19] S. Yapici, 'Electrochemical Mass transfer in Annular Swirl Flow', PhD thesis, University of Exeter, UK (1992).
[20] J. A. Brighton and J. B. Jones, *J. Basic Eng.* **86** (1964) 835.
[21] P. V. Shaw and T. J. Hanratty, *AIChE J.* **10** (1964) 475.
[22] F. P. Berger and A. Ziai, *Chem. Eng. Res. Des.* **61** (1983) 377.
[23] S. Yapici, M. A. Patrick and A. A. Wragg, *Int. Comm. Heat Mass Transf.* **21** (1994) 41.
[24] C. J. Scott and D. R. Rask, *J. Fluid Eng. Trans. ASME* **95** (1973) 557.
[25] B. R. Clayton and Y. S. M. Morsi, *Int. J. Heat Fluid Flow* **6** (1985) 31.
[26] F. M. Yowakim and R. J. Kind, *J. Fluid Eng.* **110** (1973) 257.
[27] A. Storck and F. Coeuret, *Electrochim. Acta* **22** (1977) 1155.
[28] N. A. Chigier and J. M. Beer, *J. Basic Eng. Trans. ASME* **86** (1964) 788.
[29] P. Bradshaw, AGARDograph, NASA, Langley (1973).
[30] H. Aouabed, P. Legentilhomme, C. Nouar and J. Legrand, Proceedings of the 3rd international workshop on *Electrodiffusion Diagnostics of Flows*, (edited by C. Deslouis and B. Tribollet), Dourdan, France (1993) p. 299.
[31] S. M. Chouikhi, M. A. Patrick and A. A. Wragg, *J. Appl. Electrochem.* **17** (1987) 1118.
[32] Z. Mao and T. J. Hanratty, *Experiments in Fluids* **11** (1991) 65.